In-Chain Tunneling through Charge-Density-Wave Nanoconstrictions and Break Junctions

K. O'Neill,[1,2] E. Slot,[1] R. E. Thorne,[2] and H. S. J. van der Zant[1]

[1]*Kavli Institute of Nanoscience Delft, Delft University of Technology, Lorentzweg 1, 2628 CJ Delft, The Netherlands*
[2]*Laboratory of Atomic and Solid State Physics, Cornell University, Ithaca, New York 14853, USA*

(Received 5 September 2005; published 9 March 2006)

We have fabricated longitudinal nanoconstrictions in the charge-density wave conductor (CDW) $NbSe_3$ using a focused ion beam and using a mechanically controlled break-junction technique. Conductance peaks are observed below the $T_{P1} = 145$ K and $T_{P2} = 59$ K CDW transitions, which correspond closely with previous values of the full CDW gaps $2\Delta_1$ and $2\Delta_2$ obtained from photoemission. These results can be explained by assuming CDW-CDW tunneling in the presence of an energy gap corrugation ϵ_2 comparable to Δ_2, which eliminates expected peaks at $\pm|\Delta_1 + \Delta_2|$. The nanometer length scales our experiments imply indicate that an alternative explanation based on tunneling through back-to-back CDW–normal-conductor junctions is unlikely.

DOI: 10.1103/PhysRevLett.96.096402 PACS numbers: 71.45.Lr, 73.23.−b, 73.40.Gk, 74.50.+r

Charge-density wave (CDW) conduction remains of major interest despite its experimental discovery nearly 30 years ago. Much of the existing work has focused on transport properties of as-grown single crystals [1]. More recently, micro- and nanofabrication methods for CDW materials has allowed the study of mesoscopic CDW physics [2–4]. Structures for tunneling spectroscopy are of particular interest because of the unusual gap structure with large one-dimensional fluctuation effects expected in these highly anisotropic materials, and because of predictions of unusual midgap excitations of the collective mode [5]. Tunneling studies in fully gapped CDW conductors like the "blue bronze" $K_{0.3}MoO_3$ suffer from band-bending effects at the interface akin to semiconductor-insulator-metal junctions. These effects are absent in the partially gapped CDW conductor $NbSe_3$, which remains metallic down to 4.2 K.

Tunneling perpendicular to the direction **b** of the quasi-one-dimensional chains, along which the CDW wave vector lies, has been studied in ribbonlike whiskers of $NbSe_3$ by scanning tunneling microscopy (STM) [6], by tunneling through Pb contacts evaporated over the native oxide on the *b*-*c* plane [7,8], and by tunneling through a gold wire or a $NbSe_3$ crystal that is laid across another $NbSe_3$ crystal, forming junctions in the **a**-**b** or **b**-**c** planes [9,10]. Peaks in the $T = 4.2$ K differential conductance at 35 and 101 mV [6], 35 mV [7], 36 mV and 90 mV [9], and 37 mV and 100 mV [10] from metal-$NbSe_3$ junctions correspond well with the CDW gaps $\Delta_1 = 110$ mV and $\Delta_2 = 45$ mV for $NbSe_3$'s $T_{P1} = 145$ K and $T_{P2} = 59$ K CDWs as determined by angle-resolved photo emission (ARPES) [11]. Crossed $NbSe_3$-$NbSe_3$ crystals [9] yield peak voltages of 60 mV and 142 mV, and interlayer tunneling in microfabricated $NbSe_3$ mesas yields peaks at 50 mV and 120 mV [3]. A single in-chain tunneling study [2] using a gold ribbon mechanically positioned near the end of a $NbSe_3$ crystal gave a peak at 100 mV for the T_{P1} CDW.

Here we demonstrate that a small constriction in a $NbSe_3$ single crystal, produced by dry etching with a Ga focused ion beam (FIB), shows conductance peaks at 105 mV and 190 mV corresponding to $2\Delta_1$ and $2\Delta_2$, as illustrated in Fig. 1. We reproduce the data at 4.2 K using a mechanically controlled break-junction (MCBJ) technique, demonstrating that the FIB results are not dominated by Ga ion damage. Our results can be explained by CDW-CDW tunneling in the presence of a large transverse gap corrugation, although tunneling through back-to-back CDW–normal-conductor junctions cannot be conclusively ruled out.

CDWs form in metals with quasi-one-dimensional Fermi surfaces. Electron-hole pairs near the Fermi level k_F form a macroscopic condensate and associated periodic modulations of the electron density and atomic positions. The condensate arises from the electron-phonon interaction, as described by the mean-field Hamiltonian $H_P = \sum_{k\sigma} \epsilon_k a^\dagger_{k\sigma} a_{k\sigma} - \sum_{k\sigma} (a^\dagger_{k\sigma} a_{k+k_F\sigma} \Delta e^{i\phi} + \text{H.c.})$ [12], where $a_{k\sigma}$ ($a^\dagger_{k\sigma}$) is the electron creation (annihilation) operator for the states with wave vector k and spin σ. Like conven-

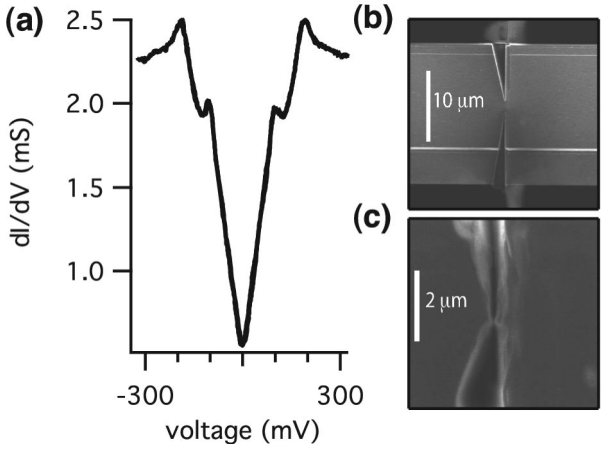

FIG. 1. (a) Differential conductance $\frac{dI}{dV}$ vs applied voltage at $T = 4.2$ K of a FIB-fabricated $NbSe_3$ nanoconstriction. (b) and (c) show images taken in the FIB during fabrication.

tional superconductors, the CDW condensate produces peaks in the density of states (DOS) at $\pm\Delta$ relative to the Fermi energy. Applying the semiconductor model for electron tunneling in superconductor junctions [13] to CDW systems, tunneling between occupied and unoccupied states in a CDW-insulating-CDW junction should produce peaks in the conductance at voltages equal to $\pm\frac{2\Delta}{e}$. In a CDW–normal-conductor junctions, peaks should be observed at voltages equal to $\pm\frac{\Delta}{e}$.

To fabricate nanoconstrictions using the FIB, a single-crystal whisker of $NbSe_3$ with a typical width of 20 μm was placed on a silicon dioxide/silicon substrate having 2 μm wide Au electrical contacts that were prepatterned by photolithographic techniques. The $NbSe_3$ crystal was then carved using an FEI–Philips FIB-200 focused ion beam. At low magnification (10 000 $\times$), two large transverse cuts were made from either side to create a constriction in the **b** direction. At high magnification (50 000 $\times$), further line cuts were made at low currents of 350 pA until the constriction had a width of around 100 nm and its resistance (which dominated the overall sample resistance) exceeded 150 Ω at room temperature. Images of both cuts, taken in the FIB, are shown in Fig. 1(b). To find the cross-sectional dimension of the junction we can make a simple estimate using the classical (diffusive) resistance formula, the contact's room temperature resistance of 165 Ω, $NbSe_3$'s bulk resistivity (1.86 Ω μm), and a contact length of around 100 nm [estimated from the device image in Fig. 1(b)], which gives a conducting area of roughly 20 nm^2.

Differential conductance versus voltage data was measured between $T_{P1} = 145$ K and 4.2 K using a conventional four-probe technique [14]. Figure 2(a) shows that the constriction's zero-bias resistance increases monotonically with decreasing temperature, and at 4.2 K has a value close to 2 kΩ. This contrasts with the bulk behavior of $NbSe_3$, which shows large resistance increases just below the two Peierls transitions and then a strong metallic (roughly linear) decrease down to 4.2 K (inset).

To fabricate constrictions by the mechanically controlled break-junction technique, a single-crystal whisker of $NbSe_3$ was placed on a Kapton-tape capped piece of flexible phosphor bronze. The crystal was held to the Kapton, which had prepatterned gold electrical contacts, using cellulose. The crystal was controllably broken at 4.2 K in a custom-built cryostat [15], which allowed the sample to be broken and recontacted several times in the course of an experiment. Transport measurements at $T =$ 4.2 K were performed in two-probe configuration, with a contact resistance of $\sim$10 Ω estimated from the total sample plus contact resistance before breaking. Because of the quasi-one-dimensional bonding and very strong bonds along the chains, the $NbSe_3$ crystal's response to stress likely involved successive breaking of fibers within its cross section, as in the breaking of a rope.

Figure 2(b) shows the differential conductance of the FIB sample as a function of voltage for several temperatures, with the lowest temperature differential conductance offset downwards for clarity. At $T = 4.2$ K, peaks occur at $\pm$105 meV and $\pm$190 meV, symmetric around zero bias, with a width $\sim$30 meV and an estimated error $\sim$6 meV. The peak positions move to smaller voltage with increasing temperature. Above its corresponding $\sim 2T_P/3$, each peak becomes an inflection, and above T_P each inflection disappears, indicating a strict association of each peak with each Peierls instability. Figure 2(c) shows the corresponding data at $T = 4.2$ K from the MCBJ sample. Peaks are clearly visible at $\pm$81 mV and $\pm$196 mV.

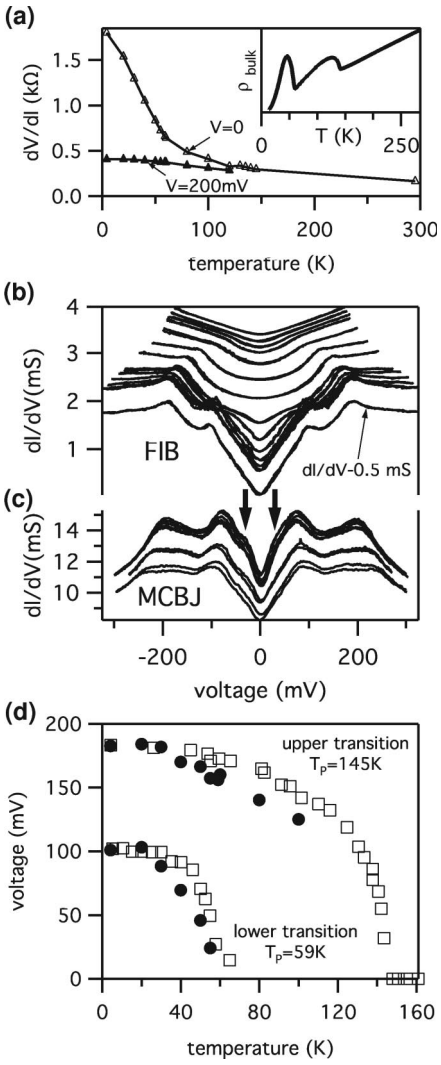

FIG. 2. (a) $\frac{dI}{dV}$ of the FIB nanoconstriction at V = 0 mV and V = 200 mV as a function of temperature. Anomalies due to the two Peierls transitions at 145 K and 59 K seen in the bulk resistivity (inset) are absent. (b) $\frac{dI}{dV}$ vs voltage of the FIB constriction at temperatures (top to bottom) of 4.2 K, 20 K, 30 K, 40 K, 50 K, 80 K, 100 K, 120 K, 130 K, 135 K, 140 K, and 145 K. The 4.2 K data are repeated, offset downward by -0.5 mS, for clarity. (c) $\frac{dI}{dV}$ vs voltage of the break-junction sample taken at different stresses or separations. (d) Temperature dependence of peak positions obtained from the FIB constriction data of (b) (filled circles) compared with x-ray diffraction experiments of the CDW order parameter [16] (open squares).

The agreement between the MCBJ and FIB samples indicates that the transport properties of the FIB samples are not qualitatively changed by any damage or disorder caused by gallium atoms. The measured $T = 4.2$ K peak positions correspond well to recent angle-resolved photoemission spectroscopy measurements of the full CDW gaps $2\Delta_1$ and $2\Delta_2$ of 90 and 220 meV, respectively, [11]. Figure 2(d) shows the position of the conduction peaks (or inflections) with temperature. Their temperature dependence closely matches that of the CDW order parameter determined from x-ray diffraction measurements [16]. Small subgap features are also observed in both the FIB and more clearly in the MCBJ samples (indicated by arrows), possibly due to soliton effects [5]. Careful analysis of Fig. 2(b) shows the absence of any feature at $\frac{\Delta_1+\Delta_2}{e} \simeq$ 145 meV, which might be expected for tunneling between the T_{P1} CDW on one side of the constriction and the T_{P2} CDW on the other.

The conductance peak widths do not significantly vary below $\frac{T_P}{2}$ for either transition, implying a temperature-independent intrinsic broadening of the CDW DOS. Down to the lowest temperatures, the conductance also shows a substantial tail as the voltage decreases below the gap, indicating that the DOS does not cut off sharply at the nominal gap energy. This is consistent with optical absorption measurements [17], and calculations of the zero-temperature CDW DOS with one-dimensional fluctuations [18]. Suppression of conductance peaks at $>2T_P/3$ for each CDW is likely due to the strong effect of thermal fluctuations on the DOS in a quasi-one-dimensional system [19].

Our results may be explained in terms of CDW-CDW tunneling in the presence of a transverse corrugation of the T_{P2} CDW's energy gap, as shown in Fig. 3. Interchain coupling results in band structure dispersion in momenta perpendicular to the chains (**b** direction), which should produce transverse corrugations in the CDW gap and imperfect nesting [20]. In $NbSe_3$, the measured electrical anisotropy implies a bandwidth in the **c** direction a factor of 10 larger than in the **a** direction, qualitatively consistent with band structure calculations [21], so that the former should dominate in tunneling involving the T_{P2} gap. Analysis of measurements on metal-$NbSe_3$ tunnel junctions at low biases [8] and of bulk low-temperature thermal and electrical conduction [22] have both suggested a transverse bandwidth comparable to the T_{P2} gap itself.

We consider a semiconductor tunneling model [13] including finite transverse dispersion in the **c** direction. This dispersion is characterized by a single parameter $\epsilon_0 = \frac{t_\perp^2 \cos(bk_F)}{2t_b \sin(bk_F)}$, $t_\perp$ and t_b being the bandwidths of the dispersion perpendicular and parallel to the chains, and b the interchain separation. Figure 3(a) illustrates this dispersion, showing by brightness the density of states $N(E, k_\perp)$ as a function of energy and perpendicular wave vector within one half Brillouin zone (left), and the density of states at a $N(E)$ at a fixed wave vector (right). The conductance is

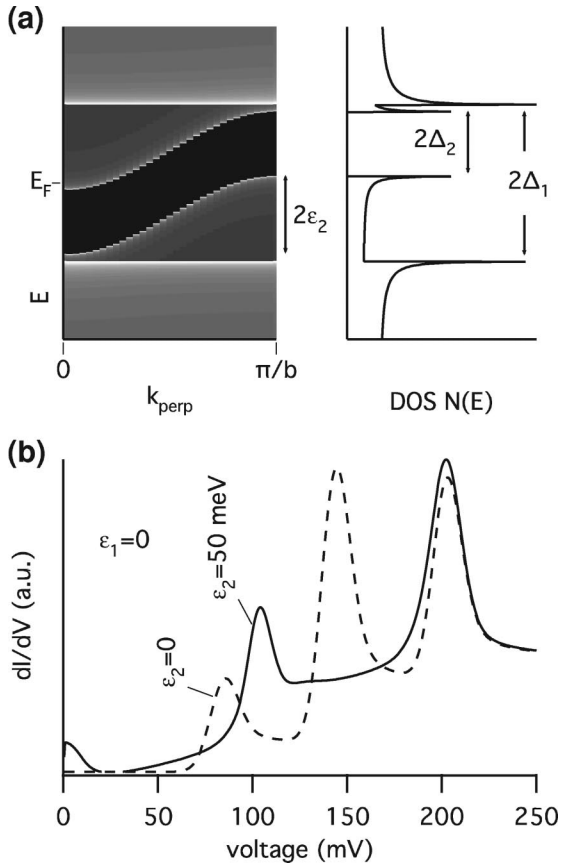

FIG. 3. Semiconductor model for transitions between quasiparticle excited states of the CDW, with corrugation ϵ_2 present in the transverse momentum direction of the $T_{P2} = 59$ K but not the $T_{P1} = 145$ K CDW states. (a) Left: density of states $N(E, k_\perp)$ as a function of perpendicular wave vector and energy, showing how corrugation of the T_{P2} CDW changes the relative positions of the DOS maxima. Brighter regions denote higher DOS. Right: projection of $N(E, k_\perp)$ at a fixed wave vector $k_\perp = \frac{\pi}{b}$. (b) Simulated $\frac{dI}{dV}$ vs V using a BCS density of states broadened by 24 meV, and corrugations $\epsilon_2 = 0$ and 50 meV. All calculations assume $\Delta_1 = 100$ meV and $\Delta_2 = 41$ meV.

then calculated by integrating the product $N(E, k_\perp)N(E - eV, k_\perp)$ over all energies E and wave vectors $k_\perp$, assuming a BCS $T = 0$ DOS broadened by a Gaussian distribution of width $\sigma = 24$ meV to mimic the experimental peak broadening. The computed $\frac{dI}{dV}(V)$ curves for $\epsilon_2 = 0$ (no corrugation) and $\epsilon_2 = 50$ meV are shown in Fig. 3(b). As expected, with no corrugation $\frac{dI}{dV}(V)$ exhibits a strong peak at $(\Delta_1 + \Delta_2)/e$. As ϵ_2 is increased, this peak splits in energy and shrinks in height. While all conductance peaks remain visible with a divergent DOS, with a broadened DOS the peaks at $\Delta_1 + \Delta_2 - \epsilon_2$ and $2\Delta_2$ merge at around 100 meV, resulting in a conductance curve that closely resembles the present data. The transverse gap corrugation we assume to obtain the best fit to our data is in agreement with the conclusion of Sorbier *et al.* [8] that the corrugation for the T_{P2} CDW ϵ_2 is slightly larger than the CDW gap Δ_2.

An alternative explanation is that the peak structure results from back-to-back normal-conductor–CDW junctions. Provided that the relaxation length of the nonequilibrium distributions is long compared with the characteristic length of the transition from CDW to normal states, one would expect $\frac{dI}{dV}$ peaks corresponding to $2\Delta_1$ and $2\Delta_2$, and no intermediate peak. We can estimate the dimensions of the constricted region from the measured behavior of $NbSe_3$ nanowires of different cross-sectional dimensions [23]. The low-field residual resistance ratio $\frac{R(T=293\ \mathrm{K})}{R(T=4.2\ \mathrm{K})}$ of our FIB constriction most closely matches a nanowire with resistance per unit length $R/L \sim 10^6\ \Omega/\mu$m at 4.2 K, corresponding to a cross section of 600 nm^2. From the measured junction resistance $R(T = 4.2K) = 1798\ \Omega$ we obtain a junction length $\sim$1.8 nm. This is comparable to the known CDW amplitude coherence length in $NbSe_3$, and is too short to allow the full loss of CDW order required to achieve the tunneling characteristics of back-to-back CDW–normal-conductor junctions. Furthermore, even the smallest cross-section nanowires (500 nm^2) studied to date show inflections in the resistance near the two Peierls transitions; the FIB constriction shows no hint of these anomalies.

The back-to-back junction interpretation might be viable if the FIB somehow disorders the constricted region in a way that eliminates the Peierls transitions and causes the resistance to increase strongly with temperature, while producing a resistivity whose magnitude is smaller than in $NbSe_3$ nanowires. But even in this case the observed zero-bias junction resistance cannot easily be accounted for [24]. In addition, the relevance of the back-to-back junction explanation to MCBJ samples, where the sample has simply been broken and brought back close together, is unclear due to the absence of an intermediate conducting structure. We therefore attribute the conductance peaks in our devices to CDW-CDW tunneling.

In conclusion, we have fabricated in-chain nanoconstrictions in a CDW material. These constrictions behave like a tunnel junctions, and conductance peaks are observed at biases that correspond well with the full CDW gaps $2\Delta_1$ and $2\Delta_2$ determined from independent measurements. The peaks disappear at around two-thirds the respective Peierls transition temperature, in agreement with calculations of the effects of fluctuations on the DOS for one-dimensional compounds.

We thank S. Zaĭtzev-Zotov and S. Artemenko for fruitful discussions. This work was supported by the International Association for the Promotion of Cooperation with Scientists from the New Independent States of the Former Soviet Union (INTAS-NIS), the Foundation for Fundamental Research on Matter (FOM), and the National Science Foundation (NSF) (Grants No. DMR 0101574 and No. INT 9812326). K. O'N. was supported by the NSF and by the Marie Curie Fellowship Association. We thank J. van Ruitenbeek for the use of equipment in the MCBJ work, and S. Otte and R. Thijssen for technical assistance.

[1] G. Grüner, Rev. Mod. Phys. **60**, 1129 (1988).
[2] A. A. Sinchenko, Y. I. Latyshev, S. G. Zybtsev, I. G. Gorlova, and P. Monceau, Phys. Rev. B **60**, 4624 (1999).
[3] Y. I. Latyshev *et al.*, J. Phys. A **36**, 9323 (2003).
[4] S. V. Zaĭtsev-Zotov, Phys. Usp. **47**, 533 (2004); S. V. Zaĭtsev-Zotov, V. Y. Pokrovski, and P. Monceau, JETP Lett. **73**, 25 (2001).
[5] S. Brazovskii, I. E. Dzyaloshinskii, and I. M. Krichever, Phys. Lett. **91A**, 40 (1982).
[6] Z. Dai, C. G. Slough, and R. V. Coleman, Phys. Rev. B **45**, R9469 (1992).
[7] A. Fournel, J. P. Sorbier, M. Konczykowski, and P. Monceau, Phys. Rev. Lett. **57**, 2199 (1986).
[8] J. P. Sorbier, H. Tortel, P. Monceau, and F. Levy, Phys. Rev. Lett. **76**, 676 (1996).
[9] T. Ekino and J. Akimitsu, Jpn. J. Appl. Phys. **26**, 625 (1987).
[10] T. Ekino and J. Akimitsu, Physica (Amsterdam) **194-196B**, 1221 (1994).
[11] J. Schäfer *et al.*, Phys. Rev. Lett. **91**, 066401 (2003).
[12] H. Fröhlich, Proc. R. Soc. London, Ser. A **223**, 296 (1954); R. E. Peierls, *Quantum Theory of Solids* (Oxford University Press, New York, 1955).
[13] G. E. Blonder, M. Tinkham, and T. M. Klapwijk, Phys. Rev. B **25**, 4515 (1982).
[14] Two other FIB samples with insulating properties showed features near $2\Delta_1$ and $2\Delta_2$. One of these had inflection points near 200 mV and 106 mV; the other had a peak at 170 mV and an inflection at $\sim$100 mV.
[15] J. M. van Ruitenbeek *et al.*, Rev. Sci. Instrum. **67**, 108 (1996).
[16] R. M. Fleming, D. E. Moncton, and D. B. McWhan, Phys. Rev. B **18**, 5560 (1978).
[17] A. Perucchi, L. Degiorgi, and R. E. Thorne, Phys. Rev. B **69**, 195114 (2004).
[18] K. Kim, R. H. McKenzie, and J. W. Wilkins, Phys. Rev. Lett. **71**, 4015 (1993); R. H. McKenzie and J. W. Wilkins, Phys. Rev. Lett. **69**, 1085 (1992).
[19] P. A. Lee, T. M. Rice, and P. W. Anderson, Phys. Rev. Lett. **31**, 462 (1973).
[20] X. Huang and K. Maki, Phys. Rev. B **42**, 6498 (1990); X. Z. Huang and K. Maki, Phys. Rev. B **40**, 2575 (1989).
[21] J. Schäfer (private communication).
[22] G. Mihály, A. Virosztek, and G. Grüner, Phys. Rev. B **55**, R13456 (1997).
[23] E. Slot, M. A. Holst, H. S. J. van der Zant, and S. V. Zaĭtsev-Zotov, Phys. Rev. Lett. **93**, 176602 (2004).
[24] The boundary between metallic and nonmetallic behavior lies at the resistivity of roughly 150 mΩ cm [J. H. Mooij, Phys. Status Solidi A **17**, 521 (1973)]. Conservatively taking the junction cross section to be 100×100 nm and the measured room temperature resistance of about 150 Ω, the constriction length would be 1 nm, which again is too small to be consistent with back-to-back tunneling.